

1 **Use of membranes and detailed HYSPLIT analyses to understand**
2 **atmospheric particulate, gaseous oxidized, and reactive mercury chemistry**

3 Mae Sexauer Gustin^{1*}, Sarrah M. Dunham-Cheatham¹, Lei Zhang², Seth Lyman³, Nicole
4 Choma¹, Mark Castro⁴

5
6 ¹ Department of Natural Resources and Environmental Science, University of Nevada, Reno, NV
7 89557, USA

8 ² School of the Environment, Nanjing University, Nanjing, Jiangsu 210023, China

9 ³ Bingham Research Center, Utah State University, Vernal, UT 84322, USA

10 ⁴ Appalachian Laboratory, University of Maryland Center for Environmental Science, Frostburg,
11 MD 21532, USA

12
13 *Corresponding author: Mae Sexauer Gustin, mgustin@cabnr.unr.edu, 001-775-784-4203

14
15
16 **Abstract**

17 The atmosphere is the primary pathway by which mercury enters ecosystems. Despite the
18 importance of atmospheric deposition, concentrations and chemistry of gaseous oxidized (GOM)
19 and particulate-bound (PBM) mercury are poorly characterized. Here, three membranes (cation
20 exchange (CEM), nylon, and polytetrafluoroethylene (PTFE) membranes) were used as a means
21 for quantification of concentrations and identification of the chemistry of GOM and PBM.
22 Detailed HYSPLIT analyses were used to determine sources of oxidants forming reactive
23 mercury (RM=PBM+GOM), GOM, and PBM). Despite the coarse sampling resolution (1-to-2
24 weeks), a gradient in chemistry was observed, with halogenated compounds dominating over the
25 Pacific Ocean, and continued influence from the marine boundary layer in Nevada and Utah with
26 a periodic occurrence in Maryland. Oxide-based RM compounds arrived at continental locations
27 via long-range transport. Nitrogen, sulfur, and organic RM compounds correlated with regional
28 and local air masses. RM concentrations were highest over the ocean and decreased moving from
29 west to east across the United States. Comparing membrane concentrations demonstrated that the
30 CEM provided a quantitative measure of RM concentrations, and PTFE membranes were useful
31 for collecting PBM. Nylon membranes do not retain all compounds with equal efficiency in
32 ambient air and an alternate desorption surface is needed.

33
34 Keywords: cation exchange membrane, nylon, criteria air pollutants, PTFE, thermal desorption,
35 UNR-RMAS

36

37

38 Introduction

39 The atmosphere is the primary pathway by which mercury (Hg) is deposited to
40 ecosystems, and this occurs via dry deposition of both gaseous elemental (GEM) and gaseous
41 oxidized (GOM) Hg compounds, with GOM being the dominant compound in wet deposition. It
42 has been demonstrated that the Tekran® speciation system, the only commercially available Hg
43 monitoring instrument for ambient air sampling, does not accurately measure GOM and
44 particulate-bound (PBM) Hg, and underestimates reactive mercury (RM=GOM+PBM) by up to
45 13 times¹⁻⁵. Thus, the Hg research community needs a method that allows for the accurate
46 quantification and identification of RM compounds.

47 The University of Nevada, Reno-Reactive Hg Active System 2.0 (RMAS) is a promising
48 technology for measuring reactive Hg (RM=GOM+PBM), GOM, and PBM in ambient air using
49 membranes as collection surfaces^{3,6}. Membranes used in this system include cation exchange
50 membranes (CEM) for quantification of RM and GOM concentrations and nylon membranes for
51 determination of RM and GOM chemistry. The RMAS has been applied for measurement of RM
52 across multiple sampling locations, and numerous lines of evidence (meteorology, chemistry of
53 compounds on membranes, back trajectory analyses, anion chemistry, criteria air pollutants)
54 have demonstrated the chemistry of RM compounds measured at Mauna Loa, HI, Reno, NV,
55 Piney Creek Reservoir, MD, and Horsepool, UT, USA, corresponded well with projected source
56 areas, meteorology, criteria air pollutants, and other ions collected on the membranes⁷(for
57 locations see graphical abstract).

58 Gustin et al. (2019)³ described a method whereby use of the three membranes could
59 allow for separating the components of RM, that is GOM and PBM (> 0.2 μm). The primary
60 focus of the Gustin et al.(2019)³ study was to compare four methods for measuring RM and

61 determine the potential for the three-membrane system applied here to provide a better
62 understanding of whether RM was gaseous or particle-bound. Detailed analyses of RM
63 chemistry and sources was not investigated in the 2019 study. For the present study, data were
64 collected in a transect across the United States with sampling sites on Hawai'i (HI) and in
65 Nevada (NV), Utah (UT), and Maryland (MD). Our main working hypothesis was that the three-
66 membrane system would provide a method of identification of GOM and PBM concentrations
67 and chemistry , and that the information developed would be useful for better understanding
68 atmospheric Hg chemistry. The second working hypothesis was since RM compounds present
69 are influenced by the oxidants in the air⁷, detailed HYSPLIT analyses associated with each
70 location would allow us to discern sources of oxidants forming RM compounds. The efficiency
71 of the membranes for collection of RM/GOM/PBM was also investigated to determine the
72 robustness and limitations of this method. This was addressed through comparison of
73 concentrations from membranes with and without upstream polytetrafluoroethylene membranes
74 (PTFE), and concentrations and chemistry associated with each fraction (GOM and PBM).

75 **Methods**

76 Sampling locations

77 Field sites for this study were the same as those discussed in Luippold et al.⁷, at which
78 only RM was measured. Locations included the Mauna Loa Observatory in Hawaii (HI) that is
79 operated by the National Oceanic and Atmospheric Administration (NOAA) (19.5392, -
80 155.5792; 3397 masl; 1 Aug 2019 to 2 Jan 2020, n = 10 2-week periods). The location in Reno,
81 Nevada (NV) was at the College of Agriculture, Biotechnology & Natural Resources Nevada
82 Agricultural Experiment Station Valley Road Greenhouse Complex (39.5375, -119.8047; 1371
83 masl; 1 Oct 2019 to 28 Jan 2020, n = 11 1-week periods and n = 4 2-week periods). The

84 Horsepool Monitoring Station, Utah (UT) (40.1434, -109.4689; 1567 m; 1 Aug 2019 to 6 Jan
85 2020, n = 11 2-week periods), operated by Utah State University, is south of Vernal, Utah and
86 Dinosaur National Monument in the Uintah Basin. The Piney Creek Reservoir location (MD) is
87 northeast of Frostburg, Maryland (39.7053, -79.0122; 769 masl; 15 Aug 2019 to 21 Nov 2019, n
88 = 6 2-week periods), and is operated by the University of Maryland Center for Environmental
89 Science.

90 The HI site is primarily influenced by air from the free troposphere and the marine
91 boundary layer⁷. The NV location is 50 m from I-80, a major interstate highway within the city
92 of Reno, and is also impacted by air from the free troposphere, San Francisco and Sacramento,
93 and the marine boundary layer⁷⁻⁹. UT is located in a remote area with oil and gas production
94 occurring in the basin, and inputs of air from the free troposphere. The MD location is in a
95 forested area downwind of coal-fired power plants⁷.

96 Based on work by Luippold et al.(2020)⁷, RM concentrations at HI > NV > UT > MD.
97 The RM chemistry at HI was dominated by halogen-based compounds, while in NV, halogen, –
98 N, and –S Hg compounds were abundant with some –O containing compounds present. At UT,
99 compounds included halogenated compounds along with –N and –O containing compounds.
100 Lastly, in MD, –N and –S RM compounds were dominant in the winter, while in the summer
101 organic compounds were more abundant.

102 Sampling system

103 Samples were collected from August 2019 to January 2020. The RMAS consists of a
104 custom-designed anodized aluminum weather shield (Deluxe Welding, Reno, Nevada) that
105 houses 6 filter packs. Sampling air velocity through each filter pack is regulated at 1 Lpm, using

106 critical flow orifices (Teledyne Technologies) and measured at the beginning and end of each
107 deployment. Two pumps (KNF P/N UN838KNI, these pumps were consistently used in this
108 project, but failed often and are not recommended for future use) were used so that if one pump
109 went offline, data were still being collected; the pumps were housed in a custom-designed pump
110 box. For more details, see Luippold et al. (2020)⁶. The RMAS typically houses triplicate two-in-
111 series CEM (Pall, 0.8 μm pore size) and nylon membranes (Sartorius, 0.2 μm pore size) in 6 total
112 dual-stage filter holders (Savillex). For this study, at the NV site two RMAS were used: one
113 following the traditional configuration, with 6 total dual-stage filter holders holding two-in-series
114 CEM ($n = 3$) and nylon membranes ($n = 3$). The second RMAS housed triple-stage filter holders
115 with a PTFE membrane (Sartorius, 0.2 μm pore size) upstream of the two-in-series CEM and
116 nylon membranes. This allowed for triplicate samples of all membrane measurements.

117 At HI, UT, and MD one RMAS was used and configured so that two CEM and one nylon
118 membrane dual-stage filter packs were deployed without a PTFE, and one CEM and two nylon
119 membrane dual-stage filter packs had upstream PTFE membranes upstream (Figure SI 1). This
120 did not allow for replication of all measurements and provided duplicate measurements for the
121 nylon membrane with the upstream PTFE and for the CEM without the upstream PTFE, and one
122 measurement for the nylon without the PTFE and for the CEM with the PTFE.

123 For this study, the two-in-series upstream and downstream CEM and nylon Hg
124 concentrations were added together and the blanks for that sampling time subtracted. Herein, the
125 terms “CEM RM” and “nylon RM” indicate data collected on these membranes with no
126 upstream PTFE; “CEM GOM” and “nylon GOM” are Hg concentrations on these membranes
127 with an upstream PTFE, while the PTFE membrane Hg data are considered PBM. CEM and
128 nylon GOM+PBM indicates the total Hg concentration for the PTFE plus the upstream and

129 downstream CEM and nylon membranes, respectively. Use of a single measurement for CEM
130 and nylon membranes was justified given the good replication observed in other studies using
131 this system^{6, 7}. At the end of each deployment, membranes were stored in 50 mL polypropylene
132 centrifuge tubes (Falcon®, Corning Inc)⁶ and shipped to UNR, frozen, and analyzed within two
133 weeks of receipt.

134 Blank membranes (n = 3) of each membrane type were collected at the start of each
135 deployment and kept in individual storage vessels at -20 °C and analyzed at the same time as the
136 corresponding samples. Downstream membranes were used to quantify breakthrough, calculated
137 as follows:

138

$$140 \quad \% \text{ breakthrough} = \frac{(\text{downstream membrane} - \text{blank})}{[(\text{downstream membrane} - \text{blank}) + (\text{upstream membrane} - \text{blank})]} \times 100$$

139

Equation 1

141 Analyses of membranes

142 Total Hg concentrations of CEM, the downstream nylon membranes, and PTFE were
143 determined following EPA Method 1631 that consists of BrCl oxidation, SnCl reduction, and
144 analyses using cold vapor atomic fluorescence spectrometry. All samples were above the method
145 detection limit (40 pg Hg).

146 Upstream nylon membranes were thermally desorbed to determine the RM compounds
147 collected on the membranes. Details of the thermal desorption system can be found in Luippold
148 et al.⁶ Briefly, a nylon membrane was placed inside a sealed Hg-free, temperature-controlled
149 oven and gradually heated from 50 to 200 °C at a rate of 2 °C min⁻¹. Volatilized RM compounds
150 are pulled through a pyrolyzer, to reduce all Hg compounds to elemental Hg, into a Tekran®
151 2537. RM compounds are released from the membrane at different temperatures (80–85 °C for

152 [–O], 90–110 °C for [–Br/Cl], 125–135 °C for [–N], 150–155 °C for [–S], and 180–190 °C for
153 organic Hg compounds), allowing for separation and determination of compounds as the sample
154 is gradually heated. Resulting thermal desorption profiles were compared to those generated by
155 thermally desorbing permeated pure GOM compounds. Solid compounds for which profiles have
156 been developed include HgBr₂, HgCl₂, HgN₂O₆•H₂O, HgSO₄, and HgO, and elemental Hg, as
157 well as methylmercury chloride directly added to membranes.¹⁰⁻¹²

158 Thermal desorption profiles were deconvoluted using the assumption that profiles for
159 specific compounds are Gaussian and compared to profiles generated from standard compounds
160 (see Luippold et al.(2020)⁷ supplemental information). Compound concentrations were
161 calculated using the integral of peak area (unit: pg) divided by the sampling volume. Compounds
162 were identified as those associated with –O, –Br/Cl, –N, –S, and –organics based on desorption
163 temperatures of the standard GOM compounds. In some cases, peaks overlapped and these are
164 designated as multiple compounds. These data must be used with the caveat that the exact
165 compounds are unknown, and it is likely there are compounds with complex formulas that
166 exhibit similar thermal desorption behavior compared to the pure compounds used here.

167 Back trajectories and statistical analyses

168 Two hundred and forty-hour back trajectory simulations were calculated using the
169 NOAA Air Resources Laboratory GDAS 1° data archive and Hybrid Single-Particle Lagrangian
170 Integrated Trajectory (HYSPLIT) model^{13,14}. Trajectories were analyzed using a gridded
171 frequency distribution method¹⁵, generating 216 trajectories per day or 51,840 hourly points.
172 There is only one day (Jan 2) that trajectories went back 8 days instead of 10, producing 41,472
173 points using the same 216 trajectories. This was done because the software does not work when
174 crossing over into a different calendar year.

175 Use of a large number of trajectories gives a general indication of source region and
176 representation of air mass transport. Trajectory residence times were calculated as the percentage
177 of total hourly trajectory points that resided in a three-dimensional source box. Defined source
178 boxes (Table SI 1) used in this study included Eurasia, East Asia, the North Pacific Ocean,
179 Canada, and continental United States. In addition, the percentage of trajectory points below the
180 boundary layer within each source box was designated as < 2 km masl. The 2 km cutoff was
181 used based on data collected in Nevada¹⁶ and over the marine boundary layer of the Pacific
182 Ocean¹⁶. Model output was visualized in ArcMap.

183 Microsoft Excel 2016 was used to calculate the source box residence times and the % <
184 and > the boundary layer, and to perform statistical analyses. At each location, the coefficient of
185 variation (CV = standard deviation ÷ mean) was calculated for replicate membrane data for each
186 deployment, as well as for the whole campaign for each membrane type. Air quality data used in
187 statistical analyses for the NV location was obtained from [https://wrcc.dri.edu/cgi-](https://wrcc.dri.edu/cgi-bin/rawMAIN2.pl?nvunrc)
188 [bin/rawMAIN2.pl?nvunrc](https://wrcc.dri.edu/cgi-bin/rawMAIN2.pl?nvunrc) (site 320310016 for 2019 and site 320310031 for December 2019
189 onward, as the site location was moved).

190 **Results and Discussion**

191 General trends

192 One of the major questions for this research was whether GOM versus PBM could be
193 differentiated using the three membranes. To address this question, CEM and nylon membranes
194 were deployed with an upstream PTFE; it was assumed that the PTFE was only acting as a
195 particle filter and not selectively sorbing Hg compounds due to its use in Hg samplers. If CEM
196 and nylon membranes were collecting PBM, then they should have similar total Hg
197 concentrations as the corresponding membrane type combined with the PTFE. Additionally, the

198 CEM and nylon GOM should be lower than the CEM and nylon alone if PBM is present. Nylon
199 and CEM RM and GOM followed the same trends for all locations (Figure S2).

200 At HI, CEM RM concentrations were $51 \pm 10\%$ greater than the nylon membranes
201 (Table 1), based on the slope of the regression line throughout this sampling campaign. Based on
202 data presented in Gustin et al.(Year?)¹² comparing membrane data with those collected with the
203 Tekran system KCl denuder in clean air , CEM and nylon membranes collected 2.4 and 1.6 times
204 more HgCl_2 compounds, respectively. For HgBr_2 compounds, nylon and CEM concentrations
205 were 1.7 and 1.6 times that of the denuder, respectively. Based on these results, the 50%
206 disparity observed in this study can be best explained by the RM compounds being primarily
207 HgCl_2 . Both nylon and CEM RM concentrations were highest in August and October then
208 decreased to ~ 35 and 150 pg m^{-3} through November and December (Figure 1; Table S2).
209 This trend is similar to that reported in Luippold et al.(Year?)⁷. Nylon GOM concentrations were
210 not significantly different from the nylon GOM+PBM concentrations and CEM GOM+PBM
211 concentrations were not significantly different from CEM GOM, indicating that little PBM was
212 present at this sampling location during the sampling campaign. PBM concentrations between
213 the two membranes were not significantly different ($p = 0.25$, single factor ANOVA) and the
214 percent PBM of total RM measured on the PTFE in front of the CEM and nylon membrane was
215 $3 \pm 3\%$ and $2 \pm 2\%$, respectively.

216 In NV, nylon RM concentrations were 16% lower than the CEM RM, if the first three
217 deployment periods in October 2019 were removed from the dataset (Table 1, based on the
218 regression slope; Figure 1). In Figure 1, the NV-1 plot contains all of the data for the sampling
219 campaign, and the NV-2 plot only displays the data from October 28, 2019 onward to provide a
220 closer look at the data with the initial higher concentration samples removed. When using all the

221 data (NV-1), the nylon:CEM RM ratio was 1.95. Membrane Hg concentrations all followed
222 similar trends, and the CEM GOM+PBM was, in general, similar to the CEM RM, while the
223 CEM GOM data were 36% lower than the CEM RM (Figure S2; Table 1). The nylon
224 GOM+PBM concentrations were 23% less than the CEM GOM+PBM concentrations, while the
225 nylon GOM were 60% lower than the CEM GOM. PBM concentrations associated with CEM
226 and nylon membranes were not significantly different, indicating that aerosol was being
227 collected on the PTFE membranes. The difference between the CEM and nylon membranes (for
228 NV 2 data) GOM and GOM+PBM were 60 versus 23 pg m^{-3} , respectively. The percent of PBM
229 relative to the nylon and CEM GOM+PBM were significantly different ($p = 0.04$, one way
230 ANOVA), and 57 ± 30 and 37 ± 19 % of total Hg concentrations measured on the membranes,
231 respectively. The reason for the greater percentage of PBM on nylon membranes relative to the
232 CEM was due to loss of RM compounds from the nylon membranes. Concentrations and trends
233 for RM reported in Luippold et al.(Year?)⁷ were similar to those observed in this study, with ~ 50
234 pg m^{-3} CEM RM, nylon RM concentrations 16% less than CEM RM, and concentrations
235 declining into the winter.

236 In UT, nylon RM concentrations were 58% lower than the CEM RM (Table 1). The CEM
237 GOM+PBM was 10% lower than the CEM RM, and GOM concentrations were 34% less than
238 the CEM RM. Nylon PBM and CEM PBM concentrations were similar, except for the October
239 16th, October 30th, and November 13th deployments, when the nylon PBM concentration was
240 higher. This indicates that the CEM RM and CEM GOM +PBM were essentially the same;
241 however this was not true for the nylon membrane losing GOM.

242 In MD, the nylon RM concentrations were 40% lower than CEM RM. CEM RM and
243 CEM GOM+PBM concentrations were, similar to NV, the same, and CEM GOM concentrations

244 were 24% lower than CEM RM. Nylon GOM+PBM concentrations were 42% higher than the
245 nylon RM and the nylon GOM was 13% higher than the nylon RM indicating better retention of
246 the compounds on the nylon membrane with the PTFE in front. The percentage of PBM relative
247 to the total GOM+PBM concentration on the nylon and CEM were not significantly different (p
248 = 0.99), with $49 \pm 34\%$ for nylon and $48 \pm 32\%$ for CEM. These values are variable given the
249 complex chemistry occurring over the sampling period.

250 The nylon:CEM RM concentration ratios reported in Luippold et al.(Year?)⁷ for HI, NV,
251 UT, and MD were 0.58, 0.73, 0.44, and 0.5, respectively, similar to this study (Table 1). In
252 general, for all locations except HI, PBM was collected on the PTFE (Table SI 2). It is
253 noteworthy that, on average, the nylon GOM+PBM concentrations, except for HI, were higher
254 than nylon RM by 37, 29, and 29% for NV, UT, and MD, indicating better retention of GOM
255 compounds on the nylon membrane when the PTFE was in place; HI nylon GOM+PBM
256 concentrations were not significantly different than nylon RM. Mean Hg concentrations on the
257 nylon membrane decreased from west to east due to the fact that mercury air chemistry was more
258 complex at the eastern sampling locations, with –O, –N, –S, and organic compounds that are not
259 efficiently retained on the nylon membrane⁷. The difference between the CEM RM and nylon
260 GOM+PBM also increased from west to east due to greater loss of GOM from the nylon
261 membranes. CEM RM and CEM GOM+PBM were similar across the sampling gradient,
262 indicating that the PTFE membrane was quantitatively retaining aerosol-based RM, as was the
263 CEM without the upstream PTFE. RM measurements using CEM are thought to be accurate
264 since they compared well with a calibrated dual channel system used to measure GOM
265 concentrations¹⁷, and retain generated RM compounds¹².

266 Thermal desorption profiles

267 Thermal desorption data must be viewed within the limitations of the current method.
268 Only select commercially available standard oxidized Hg compounds exist that can be used to
269 generate standard desorption profiles, and the resulting profiles overlap. The deconvolution
270 method allows for separating specific compounds, but the chemistry is complex and there are
271 likely multiple compounds with similar behaviors. In addition, since nylon membranes do not
272 appear to retain all compounds in ambient air with equal efficiency, though they do in charcoal
273 scrubbed air¹², the Hg chemistry derived from the method may not fully reflect actual RM
274 chemistry and concentrations. However, that said, this work provides a platform for better
275 understanding GOM and PBM chemistry that has not been possible with conventional methods,
276 given their limitations.

277 In previous work, Luippold et al.(Year?)⁷ demonstrated that RM compounds at: HI were
278 predominantly –Br and –Cl; NV were –Br/Cl, –N, –S, and organic; UT were –Br/Cl, or –O, –N,
279 and –Br/Cl; and MD were –N, –S, and organic. In this study, the compounds at HI were the same
280 (Table S3). In NV, the % of –O compounds was higher, otherwise the same compounds were
281 observed in both studies. At UT, –O compounds were present from August to October, similar to
282 NV where –O compounds were abundant in the autumn months. In October in UT, the RM
283 chemistry transitioned to halogenated compounds dominating, with some –N, –S, and organics
284 present as well. The same transition happened in NV at the end of November and was associated
285 with a shift from inputs from Eurasian sources to source areas from the Pacific Ocean, the
286 continental US, and Canada. Criteria air pollutant data showed high concentrations of NO₂ and
287 SO₂ when –N and –S compounds were predominant on the nylon membranes (November 19,
288 2019, December 10, 2019, and January 13, 2020)(Figure S3), indicating agreement between RM
289 compounds and locally measured air pollutants. However, the same was not true for –O and –

290 Br/Cl compounds that are thought to be derived from long-range transport. Together, this
291 indicates global, regional and local air chemistry are producing RM observed in northern NV.
292 Using back trajectories (Table SI 4, <https://scholarworks.unr.edu/handle/11714/7532>), high –O
293 concentrations at both NV and UT were associated with times when long-range transport was
294 prevalent. In MD, halogenated compounds were present when air passed over the Pacific Ocean
295 to MD. Air during this time period was derived from the marine boundary layer and free
296 troposphere (Table SI 4, <https://scholarworks.unr.edu/handle/11714/7532>).

297 At HI, RM chemistry was dominated by halogenated compounds, with a small amount of
298 –O, –S and –N compounds (Figure 1). In general, nylon GOM concentrations were higher than
299 the nylon RM concentrations, indicating loss on the nylon membrane without the upstream PTFE
300 (Table SI 2).

301 RM concentrations on the CEM and nylon membranes in NV were similar to the
302 GOM+PBM (Table SI 2). Based on the deconvoluted thermal desorption profile data, during
303 October there was a significant amount of –O, –N, and –S compounds with lesser amounts of
304 halogenated and organic compounds (Figure 1). After this time compounds were predominantly
305 –S, –N, and organic for both nylon RM and GOM compounds. In January, –O compounds
306 became prevalent again and were observed as nylon RM and GOM compounds.

307 At UT, PBM concentrations were low (< 10 pg m⁻³) and similar for the CEM and nylon
308 membranes (Figure SI 2). Nitrogen and –S compounds were predominant at this location
309 throughout the sampling campaign. When –N and organic compounds were present they were
310 found mostly in the RM measurements, indicating these compounds were present as PBM and
311 not GOM (cf. October and November data).

312 In MD, nylon GOM+PBM concentrations were higher than nylon GOM. CEM
313 GOM+PBM concentrations were higher than the nylon RM and nylon GOM+PBM
314 concentrations, but this varied, indicating reactions or loss occurring on the nylon membrane
315 alone. RM chemistry at this location was complex and RM compounds were not always present
316 as GOM. Data suggest that PBM consisted mostly of –O, –N, and halogenated compounds.

317 HYSPLIT results

318 HYSPLIT analyses were performed to better understand the sources of air interacting
319 with each site and how, in detail, this was reflected in the RM chemistry. At HI, the air was
320 primarily sourced from the marine boundary and the free troposphere, where halogenated
321 compounds are dominant (Tables SI 3 and 4, <https://scholarworks.unr.edu//handle/11714/7532>).
322 However, when air intersected with the continental US or Asia source boxes, some minor –O, –
323 N, –S, and organic compounds were present. For example, during the September 19th
324 deployment, 8% of the air sampled at the site was sourced from the continental US source box,
325 and –N was present as RM; however, –N was not detected as GOM, indicating –N compounds
326 were associated with the particulate fraction.

327 In NV, the first 4 sampling periods over the month of October had significant amounts of
328 –O, –N, and –S RM and GOM compounds (Table SI 4, Figure 1). During this time, trajectories
329 spent the majority of time over Eurasia, Asia, Canada, and the continental US (Table SI 4). For
330 the membranes collected November 19th, sampled air passed high over Eurasia and East Asia,
331 and then over the Pacific Ocean where 32% of the air mass coming into NV was < 2 km and
332 68% > 2 km. This air then subsided as it came into the United States. During this time, –O
333 compounds were present, as were halogens, –N, and –S compounds. The following week
334 (November 26th), the air mass intersecting NV spent much of its time at > 2 km above Eurasia,

335 Asia, and the Pacific Ocean, and more time at < 2 km when entering the continental US source
336 box; halogenated compounds were less abundant compared to the previous week. For the rest of
337 the sampling campaign at NV, the primary compounds were associated with anthropogenic
338 pollutants, and 10 to 32% of the air was associated with the Eurasian and Asian source boxes.

339 Air coming into UT primarily passed > 2 km over the Pacific Ocean and below the
340 boundary layer in the United States. Typically air sampled at this location spent <10% of time
341 over Canada; however, on October 31st the sampled air spent 42% of time over Canada, and RM
342 compounds were –O/Br/Cl and –N, while GOM compounds were primarily –Br/Cl (Table SI 4,
343 <https://scholarworks.unr.edu//handle/11714/7532>).

344 At MD, a small component of the RM was comprised of halogenated compounds for
345 each sampling period, except October 3rd when the air resided primarily < 2 km over the United
346 States and compounds were primarily –N, –S, and organic. During the other time periods, the
347 sampled air was impacted by long-range transport, with up to 6% of the trajectories originating
348 over Eurasia and East Asia, 21 to 52% over the Pacific Ocean, and 30 to 70% over Canada and
349 the United States.

350 Figure 2 contains trajectories for similar time periods for each location and a summary of
351 the compounds on the membranes. For HI, the air resided over the Pacific Ocean and RM
352 compounds were halogenated GOM. The air impacting NV was not associated with the air
353 impacting HI, and most of the air passed over the North Pacific Ocean (in both the boundary
354 layer and above) and below the boundary layer for the United States. Compounds reflected these
355 sources, with –Br/Cl compounds being PBM, –O, –S, and organic compounds being GOM and
356 PBM, and –N/S being GOM. At UT, the sampled air had more halogenated compounds and
357 more air sourced from the marine boundary layer and free troposphere. RM compounds included

358 –Br, –Cl, –N, –S, and organic, while GOM compounds were primarily –Br and –Cl based. This
359 indicates for NV and UT, –N and –S compounds were primarily PBM. At MD, trajectories were
360 similar in direction to NV and UT, indicating this was a fast traveling air mass that affected the
361 entire United States. At MD, RM compounds were –N, –S, and organic, while GOM compounds
362 were halogen based with some –S and organic compounds. This demonstrates that halogenated
363 compounds were present that were derived from the free troposphere and marine boundary layer.
364 In addition, –N, –S and organic RM compounds were PBM and likely derived from regional
365 and/or local pollution. For similar data presentation for all sites and deployments, see the
366 Supplemental Information Files (Tables SI 3 and 4,
367 <https://scholarworks.unr.edu/handle/11714/7532>).

368 Breakthrough

369 Percent breakthrough at HI was lowest relative to the other sampling sites, with mean
370 values of 6.4% for CEM RM, 3.7% for CEM GOM, and similar values of 1.7 and 1.9% (not
371 significantly different) for the nylon membranes RM and GOM, respectively. Based on thermal
372 desorption profiles, this indicated that halogenated compounds are most efficiently collected by
373 the nylon membranes. Percent breakthrough was not significantly correlated with concentrations
374 on the membranes. Less breakthrough was observed for the CEM GOM (Table SI 5).

375 In NV, breakthrough on average was 14% for the CEM RM and 28% for CEM
376 GOM+PBM. The % breakthrough for these two membrane configurations were similar from
377 October until November 11th, then breakthrough increased significantly, ranging for 6 to 35% for
378 CEM RM and 18 to 56% for CEM GOM+PBM. The highest percentage of breakthrough
379 occurred when –N and –S compounds were present. During October to November, there was a
380 high percent of –O compounds; more were associated with the nylon RM than the nylon GOM

381 measurement, indicating some –O compounds were aerosol and others were a gaseous form
382 (Figure 1). This suggests that –N and –S are not as efficiently retained by the CEM. Nylon GOM
383 percent breakthrough was often higher than for nylon RM, indicating the compounds collected
384 on the nylon membranes after the PTFE were less well retained.

385 At UT, breakthrough was not significantly different between the CEM and nylon
386 membrane RM and GOM concentrations. Breakthrough was higher from early October through
387 November, when there were –O, –N, –S, and organic compounds present. Comparable to other
388 sites and previous studies^{3,7}, less breakthrough was observed when halogenated compounds were
389 dominant.

390 Nylon GOM concentrations were greater than the nylon RM concentrations for four of
391 the six samples at MD. For these sampling periods, the chemistry was dominated by –N, –S, and
392 organic RM compounds, indicating that the nylon membrane does not have good collection
393 efficiency for these compounds. These results are further evidence to support the need for
394 development of an alternate surface for understanding RM chemistry.

395 Replication for this dataset

396 Investigation of replication is useful for understanding the ability of membranes to
397 consistently capture RM compounds. As documented in a previous study⁶, the CV for RM
398 concentrations on the CEM and nylon membranes was good ($8.2 \pm 4.7\% [n = 126]$ and $6.3 \pm$
399 $5.0\% [n = 103]$, respectively) with the RMAS. Overall, for this study the CEM CV for HI was
400 lowest (6%), while for NV, UT, and MD was 13, 10, and 18% respectively. For NV, where each
401 combination of membranes occurred in triplicate, the CEM GOM+PBM, CEM GOM, and nylon
402 RM CVs were 25, 30, and 9%, respectively. For nylon GOM+PBM, the variability was 11, 25,
403 6, and 75% for HI, NV, UT, and MD, respectively; for nylon GOM the values were 10, 28, 28,

404 and 38%, respectively. For NV, where each combination of membranes occurred in triplicate, the
405 CEM GOM+PBM, CEM GOM, and nylon RM CVs were 25, 30, and 9%, respectively. For NV,
406 where each sampling scenario occurred in triplicate, the CEM GOM+PBM, CEM GOM, and
407 nylon RM, the location with the and CVs were 25, 30, and 9%, respectively. The lowest CVs
408 were observed for HI, that has simple chemistry and little PBM, and higher CVs were associated
409 with sampling locations with more complex chemistry and/or a limited number of samples.

410 Implications

411 ~~Here we~~ This study demonstrated the use of the three-membrane system allows for the
412 quantification of PBM and GOM concentrations and identification of RM and GOM chemistry,
413 something that had not been previously possible. PBM concentrations on the PTFE upstream of
414 CEM and nylon membranes were the same, except in Nevada where the chemistry was much
415 more complex. Based on the comparison of the CEM RM and CEM GOM+PBM, the nylon
416 membrane consistently lost –S, –N, and organic compounds, regardless of the presence of the
417 PTFE. Good mass balances between the CEM RM and CEM GOM+PBM measurements
418 demonstrated reactions were not associated with the CEM and both RM and GOM are retained
419 on the CEM.

420 Despite long sampling durations (1 to 2 weeks), this work also demonstrated that PBM
421 and GOM concentrations and chemistry vary across space and time. HYSPLIT analyses support
422 that the chemistry of Hg compounds correspond with air masses associated with each location.
423 PBM concentrations in general were highest at NV, followed by MD > UT > HI; the high PBM
424 concentrations at NV correspond with its proximity to a major highway. The results of these
425 analyses are important for modelers trying to understand Hg deposition and provides information
426 that will be useful for expanding the chemical reactions in the models.

427 HYSPLIT analyses and comparison with compounds on membranes at the different
428 locations indicate that to understand RM chemistry we need to look beyond local oxidants and
429 understand the total air mass chemistry interacting with a site. As would be expected, RM
430 chemistry over the ocean was much less complex than over the continent; and Hg concentrations
431 were much higher. As we transition from west to east across the continental United States,
432 depending on the speed of the air mass, Eurasia, Eastern Asia, and oceanic air can impact the
433 entire continent.

434 This work demonstrated that the nylon membrane is not ideal for collecting and retaining
435 RM and GOM compounds, and thus an alternate surface is needed for thermal desorption. Gustin
436 et al. (Year?)¹² demonstrated that in charcoal-scrubbed air a linear relationship existed between
437 uptake by nylon membranes and KCl denuders, with retention being similar across all
438 compounds. Nylon membrane concentrations were 1.4 to 1.9 times higher than the denuder
439 indicating consistent, but higher uptake. In contrast, there was significant variability associated
440 with the CEM concentrations being higher than that measured by the denuder by 1.6 to 12.6
441 times. This indicates that in charcoal-scrubbed air, the nylon membranes retained a consistent
442 amount of each compound, while in ambient air the retention of –N, –S, and organic-based
443 compounds was less. PTFE membranes collected similar concentrations of PBM whether in front
444 of the nylon or CEM. PBM measurements indicated that –N, -S, –O, and organic forms were
445 present. Higher PBM concentrations were found at the NV location, that is adjacent to a highway
446 and downwind of San Francisco and Sacramento⁸. The method developed in this study is a step
447 forward for better differentiating between PBM and GOM concentrations and chemistry.

448 Acknowledgements

449 This work was made possible by the National Science Foundation Atmospheric Chemistry
450 Program Grant # 1700722. Special thanks to Marty Martinsen for deploying our samplers and
451 collecting samples on Mauna Loa, and Winston Luke for helping make the collaboration with
452 NOAA possible. This work could not have been done without the undergraduate students who
453 work in the Gustin lab, specifically Margarita Vargas Estrada, Samantha Leftwich, and Ben
454 Ingle. The authors thank three anonymous reviewers whose insightful comments led to a much-
455 improved paper.

456 Supplemental information consists of a document containing 5 tables and 2 figures, as well as
457 HYSPLIT model results for each deployment period for each sampling location at the following
458 URL: <https://scholarworks.unr.edu//handle/11714/7532>.

459

460 References cited

461 1. Talbot, R.; Mao, H. T.; Feddersen, D.; Smith, M.; Kim, S. Y.; Sive, B.; Haase, K.; Ambrose,
462 J.; Zhou, Y.; Russo, R. Comparison of particulate mercury measured with manual and
463 automated methods. *Atmosphere* **2011**, *2*, (1), 1-20.

464 2. Maruszczak, N.; Sonke, J. E.; Fu, X. W.; Jiskra, M. Tropospheric GOM at the Pic du Midi
465 Observatory-Correcting bias in denuder based observations. *Environmental Science &*
466 *Technology* **2017**, *51*, (2), 863-869.

467 3. Gustin, M. S.; Dunham-Cheatham, S. M.; Zhang, L. Comparison of 4 methods for
468 measurement of reactive gaseous oxidized, and particulate bound mercury.
469 *Environmental Science and Technology* **2019**, *53*, (24), 14489-14495. DOI
470 10.1021/acs.est.9b04648.

471 4. McClure, C. D.; Jaffe, D. A.; Edgerton, E. S. Evaluation of the KCl denuder method for
472 gaseous oxidized mercury using HgBr₂ at an in-service AMNet site. *Environmental*
473 *Science & Technology* **2014**, *48*, 11437-11444.

474 5. Lyman, S. N.; Cheng, I.; Gratz, L. E.; Weiss-Penzias, P.; Zhang, L. M. An updated review of
475 atmospheric mercury. *Science of the Total Environment* **2019**, *707*, 135575.
476 doi.org/10.1016/j.scitotenv.2019.135575.

477 6. Luippold, A.; Gustin, M. S.; Dunham-Cheatham, S. M.; Zhang L. Improvement of
478 quantification and identification of atmospheric reactive mercury. *Atmospheric*
479 *Environment* **2020a**, *224*, 117307.

480 7. Luippold, A.; Gustin, M. S.; Dunham-Cheatham, S. M.; Castro, M.; Luke, W.; Lyman, S.;
481 Zhang, L. Use of multiple lines of evidence to understand reactive mercury
482 concentrations and chemistry in Hawai'i, Nevada, Maryland, and Utah, USA.
483 *Environmental Science & Technology* **2020b**, *54*, 7922-7931.

484 8. Fine, R.; Miller, M. B.; Burley, J. Jaffe, D. A.; Pierce, R. B.; Lin, M-Y. Variability and
485 sources of surface ozone at rural sites in Nevada, USA: Results from two years of the
486 Nevada Rural Ozone Initiative. *Science of the Total Environment* **2015**, *530*, 471-482.

487 9. Pierce, A. M.; Gustin, M. S.; Christensen, J. N.; Loria-Salazar, S. M. Use of multiple tools
488 including lead isotopes to decipher sources of ozone and reactive mercury to urban and
489 rural locations in Nevada, USA. *Science of the Total Environment* **2018**, *615*, 1411-1427.

490 10. Gustin, M. S.; Pierce, A. M.; Huang, J. Y.; Miller, M. B.; Holmes, H. A.; Loria-Salazar, S.
491 M. Evidence for different reactive Hg sources and chemical compounds at adjacent
492 valley and high elevation locations. *Environmental Science & Technology* **2016**, *50*, (22),
493 12225-12231.

494 11. Huang, J. Y.; Miller, M. B.; Weiss-Penzias, P.; Gustin, M. S. Comparison of gaseous
495 oxidized Hg measured by KCl-coated denuders, and nylon and cation exchange
496 membranes. *Environmental Science & Technology* **2013**, *47*, 7307-7316.

497 12. Gustin, M. S.; Amos, H. M.; Huang, J.; Miller, M. B.; Heidecorn, K. Measuring and
498 modeling mercury in the atmosphere: A critical review. *Atmospheric Chemistry and*
499 *Physics* **2015**, *15*, 5697-5713.

500 13. Draxler, R. R.; Hess, G. D. An overview of the HYSPLIT_4 modelling system for
501 trajectories, dispersion and deposition. *Australian Meteorological Magazine* **1998**, *47*,
502 (4), 295-308.

503 14. Stein, A. F.; Draxler, R. R.; Rolph, G. D.; Stunder, B. J. B.; Cohen, M. D.; Ngan, F. NOAA's
504 HYSPLIT atmospheric transport and dispersion modeling system. *Bulletin of the*
505 *American Meteorological Society* **2015**, *96*, 2059-2077.

506 15. Weiss-Penzias, P.; Gustin, M. S.; Lyman, S. N. Observations of speciated atmospheric
507 mercury at three sites in Nevada: Evidence for a free tropospheric source of reactive
508 gaseous mercury. *Journal of Geophysical Research* **2009**, *114*, D14302.
509 doi:10.1029/2008JD011607.

510 16. Winning, T. E.; Chen, Y. L.; Xie, F. Q. Estimation of the marine boundary layer height over
511 the central North Pacific using GPS radio occultation. *Atmospheric Research* **2017**, *183*,
512 362-370.

513 17. Lyman, S.; Gratz, L.; Dunham-Cheatham, S. M.; Gustin, M. S.; Luippold, A. Improvements
514 to the accuracy of atmospheric oxidized mercury measurements. *Environmental Science*
515 *& Technology* (revision submitted).

516

518 Table 1. Top panel is mean concentration on membranes for each field location for the entire
 519 campaign, in pg m^{-3} . Bottom panel is slope and r^2 , in parenthesis, for the regression between
 520 various membrane configurations. CEM and nylon membrane measurements were made
 521 simultaneously.

522

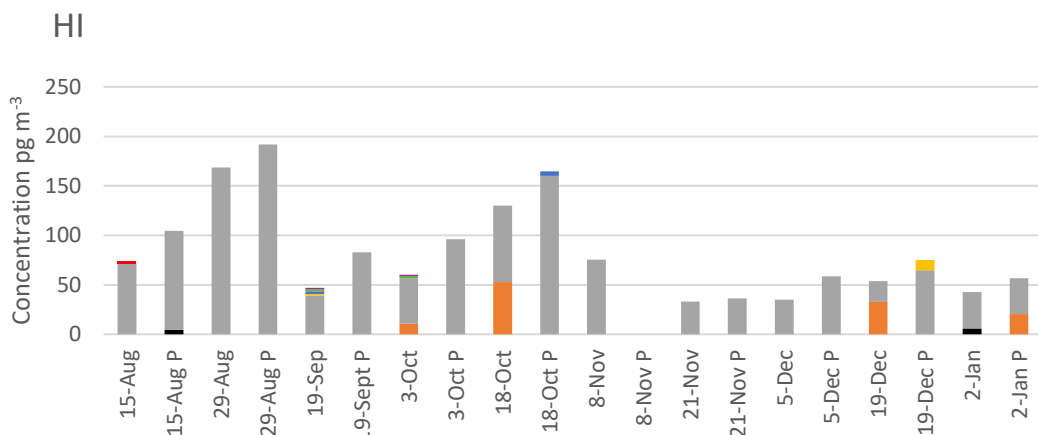
Location	HI	HI-CV	NV	NV-CV	UT	UT-CV	MD	MD-CV
<i>Number of samples</i>	10		15		11		6	
Mean (Std) concentration for entire campaign								
CEM RM	158 ± 9	0.06	32 ± 4	0.13	40 ± 4	0.10	11 ± 2	0.18
CEM GOM+PBM	168		36 ± 9	0.25	28		8	
CEM GOM	172		23 ± 7	0.30	32		12	
NYL RM	71		23 ± 2	0.09	19		5.7	
NYL GOM+PBM	102 ± 11	0.11	12 ± 3	0.25	17 ± 1	0.06	4 ± 3	0.75
NYL GOM	106 ± 11	0.10	25 ± 7	0.28	25 ± 7	0.28	8 ± 3	0.38
Slope (r2) with intercept set to zero								
CEM GOM+PM:CEM RM	1.10 (0.92)		1.1 (0.55)		0.90 (0.95)		0.98 (0.94)	
CEM GOM:CEM RM	1.09 (0.91)		0.70 (0.66)		0.66 (0.89)		0.76 (0.95)	
NYL RM:CEM RM	0.49 (0.82)		1.95 (0.3)		0.58 (0.86)		0.40 (0.69)	
NV 2 RM outliers removed								
NYL GOM+PBM:CEM RM	0.69 (0.78)		0.77 (0.84)		0.82 (0.92)		0.82 (0.92)	
NYL GOM: CEM RM	0.67 (0.81)		0.40 (0.58)		0.53 (0.84)		0.53 (0.84)	

Note mean and std are mean of 2 to 3 membranes and mean of std associated replicates

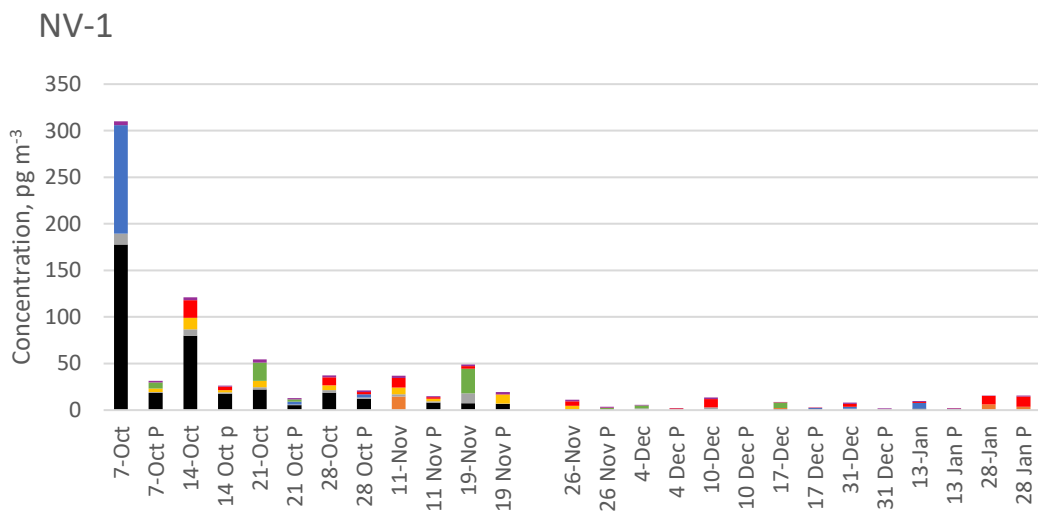
All regressions are significant at $p < 0.05$.

523 CV indicates the mean coefficient of variation for all samples.

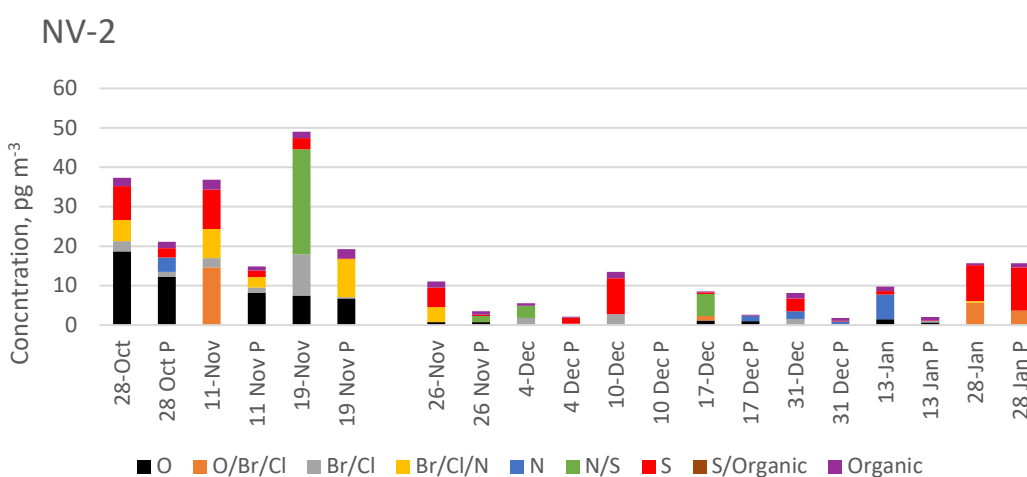
524

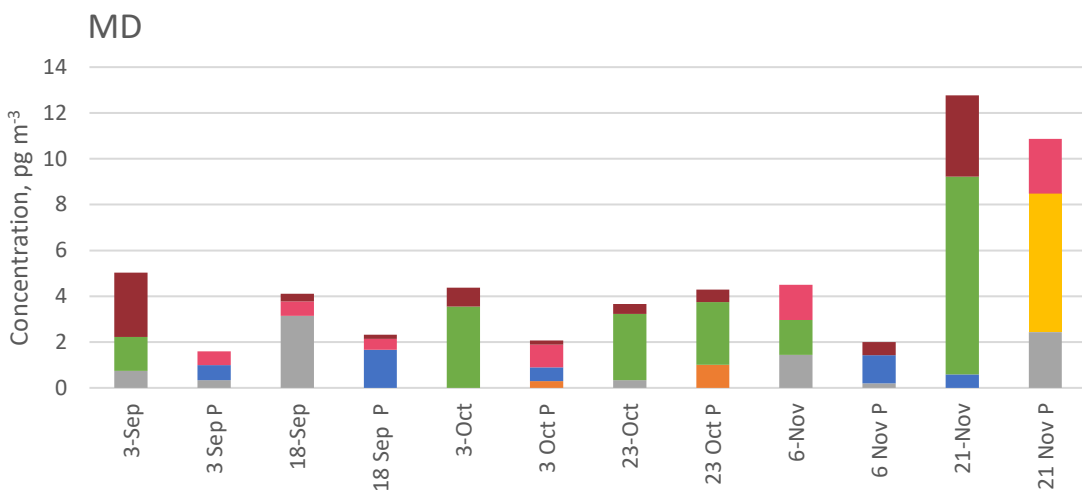
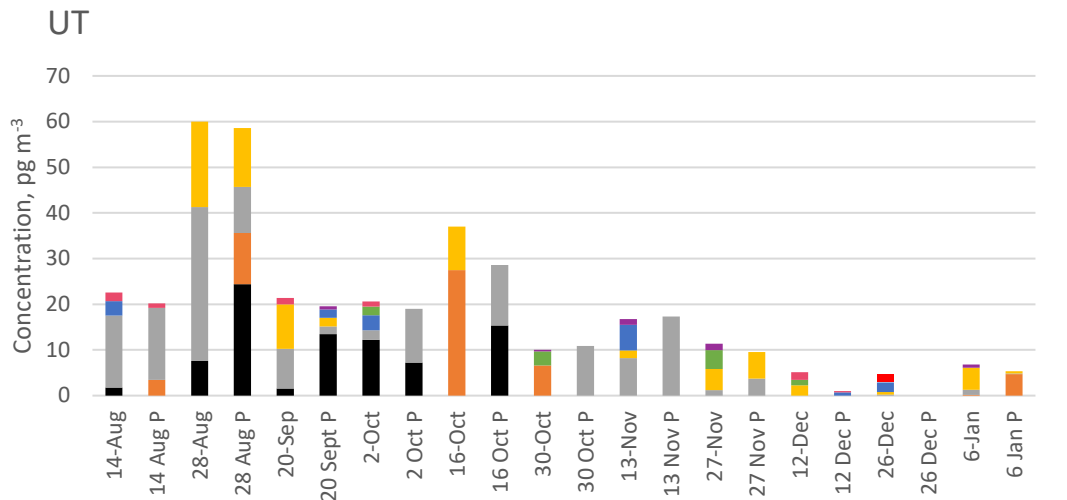


525

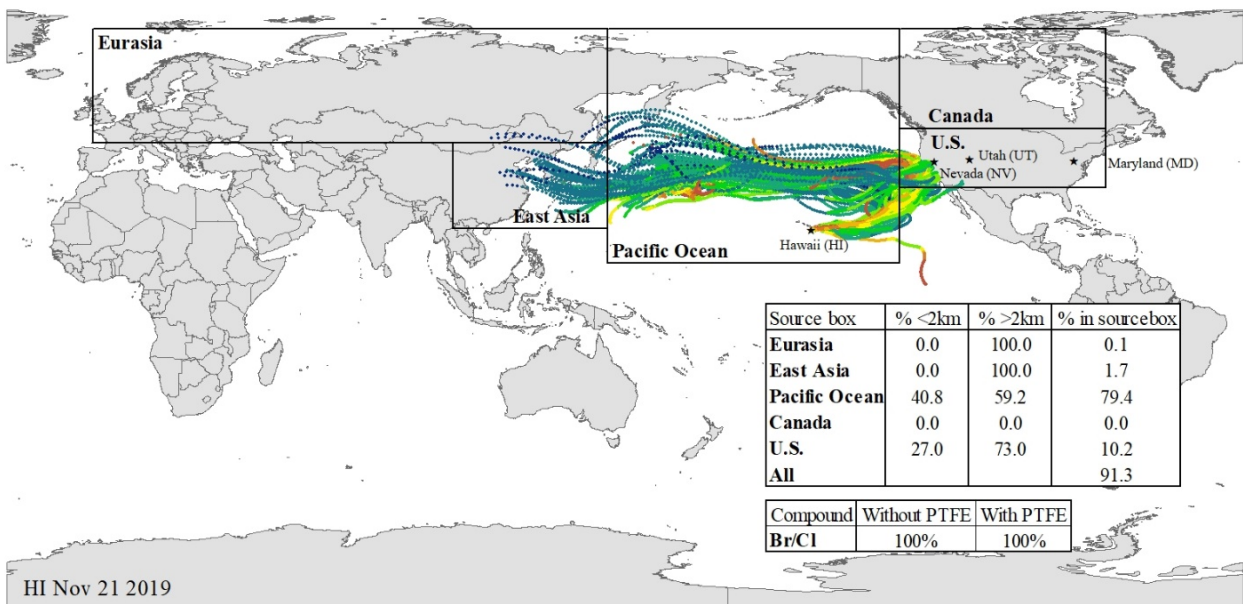


526

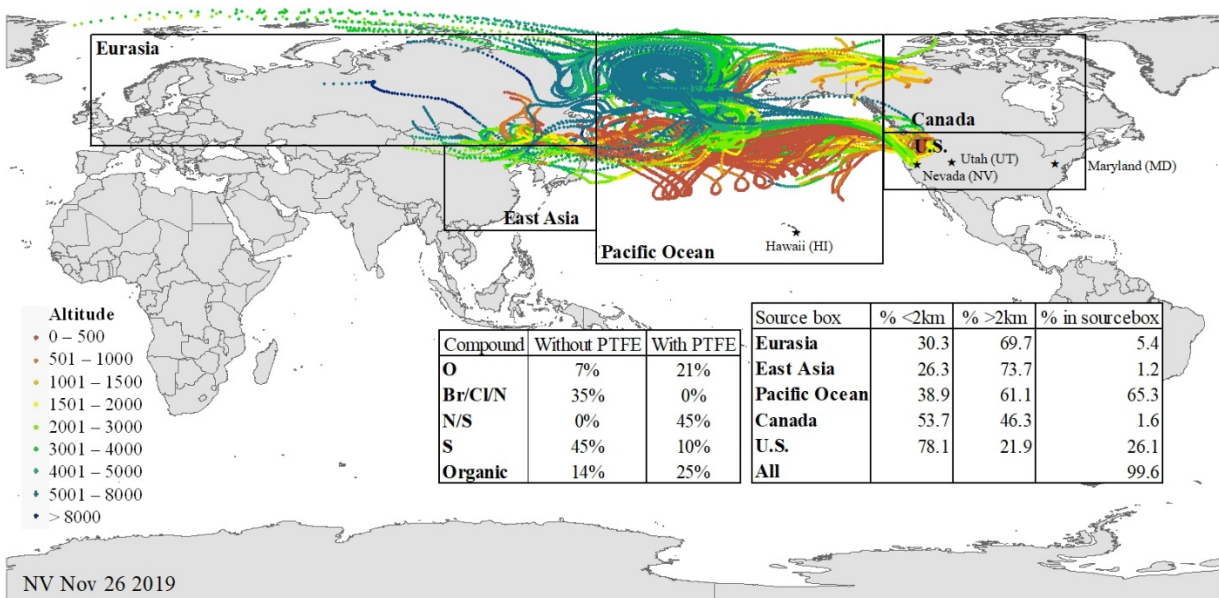




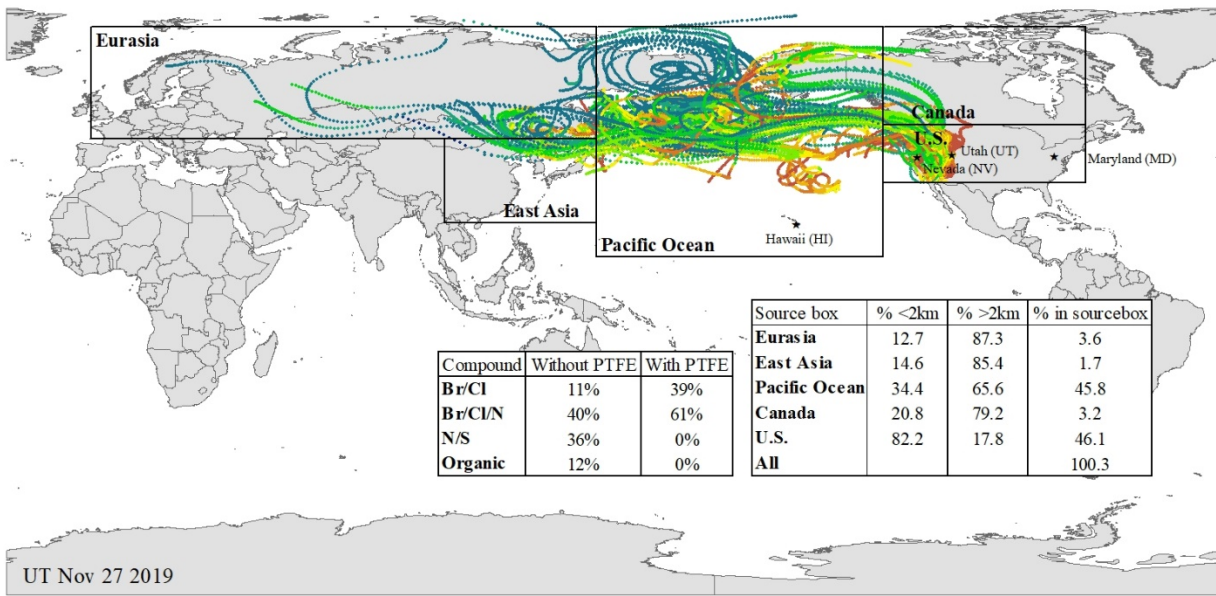
529 Figure 1. Concentrations of RM and GOM compounds on nylon membranes for each sampling
 530 deployment for each sampling location. Dates represent the end date of the deployment period.
 531 NV-2 shows the same data for NV-1, leaving out the 3 high initial sampling durations to provide
 532 a closer look at the remaining data.



533

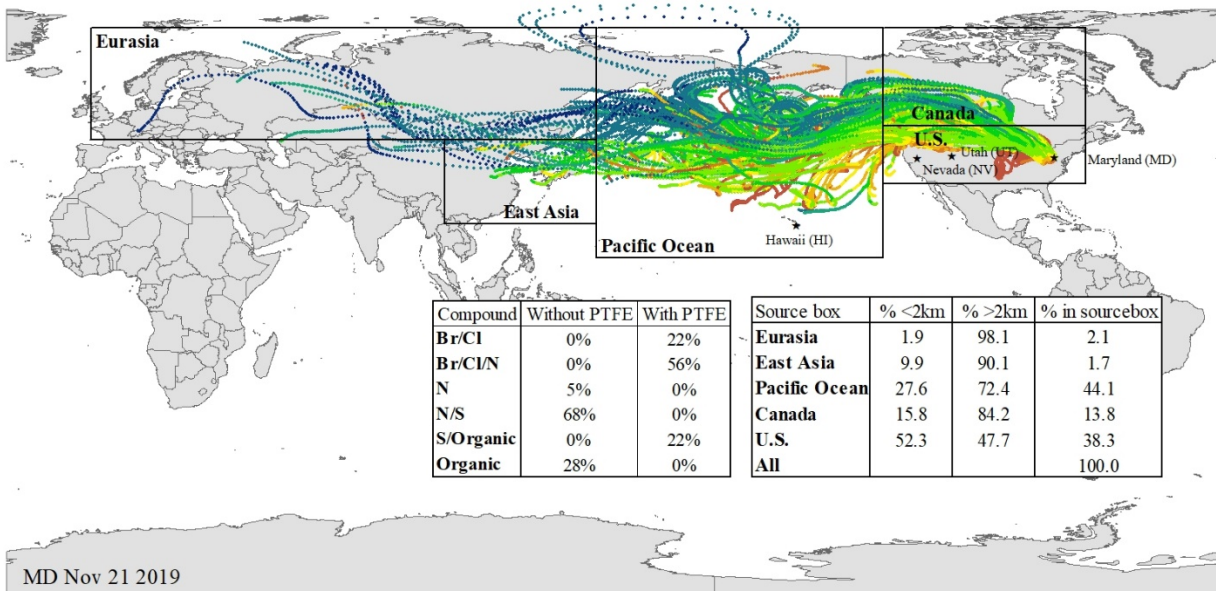


534



535

536



537

538 Figure 2. HYSPLIT trajectory analyses for the four sampling locations during a time period with
 539 overlap (see harvest dates on each map). Compounds on nylon membranes without (RM) and
 540 with (GOM) PTFE membranes are identified, as well as percent time in specific source boxes
 541 and the time above and below 2 km. The total percentage in all source boxes < 100% indicates
 542 trajectory points occurred outside of the source boxes.